International Journal of Minerals, Metallurgy and Materials
Volume 30, Number 6, June 2023, Page 1038
https://doi.org/10.1007/s12613-022-2580-7

A novel cationic collector for silicon removal from collophane using reverse flotation under acidic conditions

Zhongxian Wu[1,2,3], *Dongping Tao*[1)✉], *Youjun Tao*[2,3)✉], *Man Jiang*[1)], *and Patrick Zhang*[4)]

1) School of Resources and Environmental Engineering, Shandong University of Technology, Zibo 255049, China
2) Key Laboratory of Coal Processing and Efficient Utilization of Ministry of Education, China University of Mining & Technology, Xuzhou 221116, China
3) School of Chemical Engineering and Technology, China University of Mining & Technology, Xuzhou 221116, China
4) Florida Industrial and Phosphate Research Institute, Florida Polytechnic University, Florida 33830, USA
(Received: 2 September 2022; revised: 28 November 2022; accepted: 1 December 2022)

Abstract: We analyzed a novel cationic collector using chemical plant byproducts, such as cetyltrimethylammonium bromide (CTAB) and dibutyl phthalate (DBP). Our aim is to establish a highly effective and economical process for the removal of quartz from collophane. A micro-flotation test with a 25 mg·L^{-1} collector at pH value of 6–10 demonstrates a considerable difference in the floatability of pure quartz and fluorapatite. Flotation tests for a collophane sample subjected to the first reverse flotation for magnesium removal demonstrates that a rough flotation process (using a 0.4 kg·t^{-1} new collector at pH = 6) results in a collophane concentrate with 29.33wt% P_2O_5 grade and 12.66wt% SiO_2 at a 79.69wt% P_2O_5 recovery, providing desirable results. Mechanism studies using Fourier transform infrared spectroscopy, zeta potential, and contact angle measurements show that the adsorption capacity of the new collector for quartz is higher than that for fluorapatite. The synergistic effect of DBP increases the difference in hydrophobicity between quartz and fluorapatite. The maximum defoaming rate of the novel cationic collector reaches 142.8 mL·min^{-1}. This is considerably higher than that of a conventional cationic collector.

Keywords: cationic collector; collophane; defoaming; quartz; reverse flotation

1. Introduction

As a non-renewable resource, phosphate rock is a crucial chemical mineral, and its products are widely used in industry, agriculture, food, national defense, and other fields [1]. The use of phosphate rock has increased tremendously with rapid economic development [2]. Therefore, rational mining and efficient utilization of phosphate rock resources are necessary [3].

China has the second largest phosphate rock deposits in the world, but the average grade of its raw ore is approximately 17wt% [4]. Sedimentary collophane accounts for more than 80wt% of the total phosphate and siliceous ores. However, magnesian collophane accounts for approximately half of the majority of low- and middle-grade ore [5]. Therefore, focused research on separating low- and middle-grade siliceous and magnesian collophane from the phosphate rock deposits in China is essential. The main useful minerals obtained from collophane are phosphate minerals (apatite and fluorapatite), and gangue minerals primarily include carbonate minerals, quartz, and silicate minerals [6–7]. This type of low-grade collophane is also characterized by complex structure, fine dissemination grain size, and difficult liberation [8]. This results in complex mineral processing flowsheets, causing immense difficulties in its mining and utilization.

Low- and middle-grade siliceous and magnesian collophane are beneficiated using the double reverse flotation process [9]. This process comprises the first and second reverse flotations. In the first reverse flotation, carbonate gangue minerals are floated with a fatty acid collector under weakly acidic conditions (pH: 5.5–6.0). In the second reverse flotation, siliceous gangue minerals are floated with a cationic collector under weak alkaline conditions (pH: 9–10). However, the major problem of the double reverse flotation process is the substantially different pH requirements for the two flotation processes. Hence, a large amount of alkaline pH regulator is required in the second reverse flotation, increasing the process's complexity and cost. In addition, the cationic collector used for desilication flotation results in an overly stable froth, making defoaming difficult. Recently, the new flotation process, equipment, and collectors used for the beneficiation of low- and middle-grade collophane have achieved promising results. Amirech *et al.* [9] investigated a mixed amine collector for collophane desilication by reverse flotation at pH value ranging from 7.8 to 8.5 and obtained a concentrate with 30.1wt% P_2O_5 grade and 94wt% recovery. Du *et al.* [10] developed a closed-circuit flotation process using a sedimentation desliming step for effective magnesium removal and desilication to achieve high flotation perform-

✉ Corresponding authors: Dongping Tao E-mail: dptao@qq.com; Youjun Tao E-mail: tyj05160@163.com

ance. Liu *et al.* [11] proposed a method to control and optimize the foam stability that improved the concentrate grade by 3.93wt% and reduced the foam volume of tailings. Using a flotation column produced a concentrate with 28.28wt% P_2O_5 grade and 82.14wt% P_2O_5 recovery [12]. Currently, the double reverse flotation process for collophane beneficiation offers good performance, a short flotation process, and low collector consumption. Meanwhile, the first reverse flotation process for magnesium removal in a double reverse flotation flowsheet has been well-developed with great success. However, the second reverse flotation step for desilication has not achieved satisfactory results.

To address these problems, a novel cationic collector (KDJ) has been developed for the reverse flotation of collophane for desilication. The collecting efficacy and selectivity of KDJ were evaluated through flotation tests using pure minerals and ore samples. The interaction mechanisms between the collector and minerals were systematically examined through infrared spectrum analysis and contact angle (CA) measurements. In addition, the flotation froth produced when using KDJ was characterized through froth stability tests. The results of our study are crucial for the efficient utilization of low- and middle-grade siliceous and magnesian collophane resources.

2. Experimental

2.1. Materials and reagents

The pure quartz and fluorapatite minerals and actual collophane ore samples were acquired from a plant of Yunnan Yuntianhua Co., Ltd. (Kunming, China). The hand-picked samples of pure quartz and fluorapatite minerals were crushed using a jaw crusher (MPE-100 × 125, Jilin Exploration Machinery Plant, China) and ground to −74 μm using a mill (XPM-ϕ120 × 3, Jilin Exploration Machinery Plant, China). The ground samples were screened to obtain 38–74 μm particles for microflotation tests and −38 μm particles for Fourier transform infrared spectroscopy (FTIR) analyses.

A 7.0 kg representative finely crushed sample of the actual collophane ore was collected daily from the plant crushing site for one week, and the total sample collected was approximately 50 kg. After mixing and homogenizing thoroughly, the collected samples were divided into 300 g each and stored in sealed bags for later usage. A 300 g sample was placed in a ball mill (XMB-ϕ200 × 240; Jilin Exploration Machinery Plant, China) for each grinding test at a slurry solid concentration of 60wt% to produce a flotation feed with 88wt% particles −74 μm.

The chemical reagents used for this study are listed in Table 1. Deionized water was used in the microflotation test, and tap water (Anshan, Liaoning, China) was used in the mineral flotation test.

The KDJ collector (Table 1) was a mixture of two chemical plant byproducts artificially mixed in a mass ratio of 5:1. Further purification of these two byproducts has low economic value and is costly. However, they contain high concentrations of flotation reagent components. The main effective components in the collector were cetyltrimethylammonium bromide (CTAB) and dibutyl phthalate (DBP). Fig. 1 shows the FTIR spectra obtained by the KDJ collector. A peak at approximately 3377.71 cm^{-1} corresponded to the stretching vibration of –OH attributed to hydrogen bonds associated with the residual water in the collector [13]. The peak located at 1419.64 cm^{-1} was due to the stretching vibration of C–N, indicating that the KDJ collector was a cationic amine collector.

Table 1. Flotation reagents

Name	Application	Specification	Manufacturer
Hydrochloric acid	pH regulator	AR	Sinopharm chemical reagent Co., Ltd. (Beijing, China)
Sodium hydroxide	pH regulator	AR	Aladdin (Shanghai, China)
Sodium hexametaphosphate	Depressant	AR	Sinopharm chemical reagent Co., Ltd. (Beijing, China)
Sodium oleate	Dolomite collector	AR	Aladdin (Shanghai, China)
KDJ	Quartz collector	Industrial grade	Made in laboratory

Note: AR–analytical reagent.

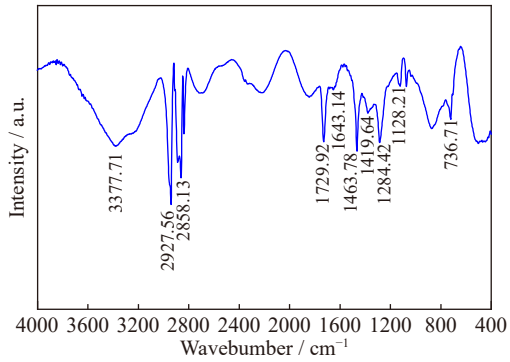

Fig. 1. Infrared spectra of collector KDJ.

The stretching vibration peaks of C=O and C–O appeared at 1729.92 cm^{-1} and 1128.21 cm^{-1}, respectively, indicating the existence of ester groups in the molecular structure of the KDJ collector. The peak at 1643.14 cm^{-1} was assigned to the stretching vibration of a benzene ring. The peak at 1284.42 cm^{-1} was caused by the wagging vibration of C–H on the benzene ring and the stretching vibration of C–C, where the benzene ring was connected with C=O. These three peaks indicate the location of the ester group on the benzene ring, providing details regarding the molecular structure of the ester compound. The remaining peaks were characteristic of carbon chains. Typical peaks of hydrocarbon chain groups

were observed at nearly 2858.13 cm^{-1} and 2927.56 cm^{-1} for symmetric and antisymmetric stretching vibration peaks of C–H, respectively [14]. The peaks at 1463.78 cm^{-1} and 736.71 cm^{-1} corresponded to the bending vibration peak of C–H and the wagging vibration peak of $–CH_2–$ (quantity of methylene group $n > 4$), respectively, indicating a long carbon chain in the collector molecule. The KDJ collector contained a long carbon chain amine compound with the benzene ring, ester group, and polymethyl group.

2.2. Methods

2.2.1. Characterization

The chemical composition of pure minerals was qualitatively characterized using an X-ray diffractometer (XRD, D8 Advance; Bruker, Germany) at 40 kV, 44 mA, and 2°/min scan rate. The test data were analyzed using the Highscore software. The multi-element analysis of pure minerals was performed using an X-ray fluorescence spectrometer (XRF, Zetium; Malvern Panalytical Company, Netherlands).

Quantitative mineralogical characterization of a collophane ore sample was performed using the automatic mineral identification and characterization system (AMICS) (Sigma 500; ZEISS, Germany). To ensure characterization efficiency and accuracy, a homogenized sample of 100 g was screened using 53 μm and 30 μm standard sieves to generate three-size fractions, namely +53, −53+30, and −30 μm, and the yield of each size fraction was determined. A 3 g sample of each size fraction was thoroughly mixed and cured with a 5 g mixture of epoxy resin (4.4 g) and curing agent (0.6 g). The cured sample was polished using a metallographic sample polishing machine. Subsequently, it was sprayed with carbon particles using an ion sputtering evaporator to ensure good conductivity on the sample surface. An AMICS analysis of the sample was conducted under an X-ray mapping measurement mode at 255 times magnification with an analytical working distance of 10.82 mm for the measurement accuracy of 0.56 μm per pixel. During measurements, the probe current was maintained at 10 nA, and the overall electron beam accelerating voltage was 20 kV. Image gray-level calibration of back-scattered electrons (BSE) was set with epoxy as the background (BSE gray value < 35) and gold metal as the upper limit (BSE gray value > 255).

2.2.2. Microflotation tests

The floatability of fluorapatite and quartz was investigated in a modified Hallimond flotation tube. A Hallimond tube is a flotation device often used for pure minerals that require a small sample size and is characterized by high efficiency, good data reliability, and reproducibility [15]. Hence, it is suitable for the preliminary screening of reagents. The Hallimond flotation tube can accurately evaluate the effect of flotation reagents on the flotation performance of minerals. Further, it can simulate the separation performance for actual minerals by the controlled blending of pure minerals.

Each microflotation test was conducted with 1.4 g pure mineral added into 5 mL deionized water in a 10 mL beaker and stirred for 3 min. Hydrochloric acid (HCl) or sodium hydroxide solution (NaOH) was added to adjust the slurry pH. A pre-determined amount of reagent was added to the pulp and conditioned for 3 min before the pulp was transferred to the Hallimond tube. After 50 mL of deionized water at the same pH value as the pulp was added and stirred for 2 min, the flotation test was initiated and continued for 3 min. The flotation products were separately filtered, dried, and weighed to calculate flotation recovery.

2.2.3. Actual mineral flotation test

Low- and middle-grade siliceous and magnesian collophane ores are generally beneficiated using a double reverse flotation process. To ensure the consistency of the process used in this study with the actual double reverse flotation process, the first reverse flotation (hereinafter called rough flotation) was carried out to remove magnesium from collophane. The concentrate from this flotation process was used as the feed to the second reverse flotation to remove silicon (hereinafter called clean flotation). Fig. 2 presents the flowsheet of the actual mineral flotation process.

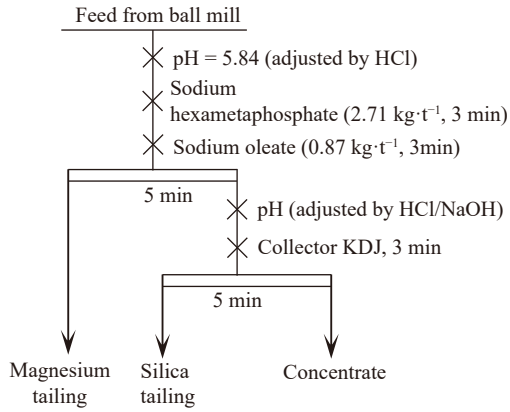

Fig. 2. Actual mineral flotation process flowsheet.

The rough flotation test was performed under the following conditions: pH value of 5.84 (adjusted by HCl), room temperature of 20°C, solid concentration of 30wt%, sodium hexametaphosphate dosage of 2.71 $kg·t^{-1}$ conditioned for 3 min, sodium oleate dosage of 0.87 $kg·t^{-1}$ conditioned for 3 min, rotation speed of 2000 r/min for the rotor of the mechanil cell, flotation aeration by natural aspiration, and flotation time of 5 min. The rough flotation produced a concentrate with 26.53wt% P_2O_5, 0.54wt% MgO, and 16.38wt% SiO_2 at a yield of 70.5wt%.

For the second reverse flotation for silicon removal, silicon removal reagent was directly added to the rough flotation concentrate slurry. The baseline flotation conditions were pH value of 6.0, solid concentration of approximately 21wt% (determined by rough flotation), and silicon removal reagent of 0.4 $kg·t^{-1}$ conditioned for 3 min. The other conditions were the same as those of rough flotation. For performance evaluation, flotation concentrate and tailing were dried, weighed, sampled, and assayed for P_2O_5 and SiO_2 contents.

All flotation tests with the actual mineral sample were performed with an XFD-III mechanil agitation flotation cell with a volume of 1 L, similar to the well-known Denver flotation machine. The device was manufactured by Jilin Exploration Machinery Co., China.

2.2.4. Zeta potential measurements

Zeta potential measurements were conducted by using a zeta potential analyzer (Stabino II, Particle Metrix, Germany). A 50 mL of suspension containing 10wt% solids, adjusted to the desired pH value with HCl or NaOH solution, was stirred for 2 min. The zeta potential was measured after 50 mg·L^{-1} of CTAB, or the KDJ collector was added into the pulp and conditioned for 3 min. The measurements were conducted at room temperature (25°C), and the average zeta potential values for at least three independent measurements were recorded.

2.2.5. Infrared spectroscopic characterization

Reagent adsorption on the surface of fluorapatite and quartz was characterized using the FTIR apparatus VERTEX-70 (Bruker, Germany). A 4.0 g pure mineral sample was conditioned in 40 mL deionized water or 25 mg·L^{-1} collector solution at pH = 6 for 10 min. Then, the conditioned suspension was filtered and washed thrice with deionized water, and the filtration cake was dried in a vacuum drying oven at 40°C. The KDJ collector or dried mineral samples were thoroughly mixed with KBr powder and ground to −5 μm in an agate mortar. The FTIR spectra were recorded in the wavenumber range of 4000–400 cm^{-1} at room temperature.

2.2.6. CA measurements

A CA measurement apparatus (JC2000C1, Powereach, China) was used to measure the CA of fluorapatite and quartz before and after interactions with different collectors. The instrument was based on the pendant drop method similar to the device used by Sadeghinezhad *et al.* [16]. The measurement procedure is as follows.

Cubic sample blocks (1 cm × 1 cm × 1 cm) with a smooth surface obtained by polishing with 400, 800, 1200, 2000, and 3000 mesh sandpapers and flannelette were conditioned in 50 mL deionized water or collector solution, with a concentration of 25 mg·L^{-1} at pH = 6 for 5 min. A drop of deionized water was placed on the sample surface using a capillary with a diameter of 0.5 mm. Image acquisition was initiated to measure the CA after the droplet became stable. The measurements were performed at room temperature, and the reported results represented the average of three repeated measurements.

2.2.7. Flotation froth stability (defoaming) test

The 163 mL froth products obtained from desilication flotation of collophane under optimum conditions (pH value of 6.0 and KDJ dosage of 0.4 kg·t^{-1}) were transferred to a 500 mL cylinder. The froth volume was measured and analyzed as a function of time. The tests were repeated three times, and the defoaming rate was the average value of the three identical tests.

3. Results and discussion

3.1. Characterization

Fig. 3 and Table 2 present the XRD data and multi-element analysis results of pure minerals, respectively. The XRD analysis results of pure minerals are consistent with the standard diffraction peaks of pure quartz and fluorapatite. The table also presents the multi-element analysis results of pure minerals. The quartz and fluorapatite samples used in this study contained 99.37wt% SiO_2 and 96.52wt% P_2O_5, respectively. Therefore, these samples were appropriate to use as pure minerals in microflotation tests.

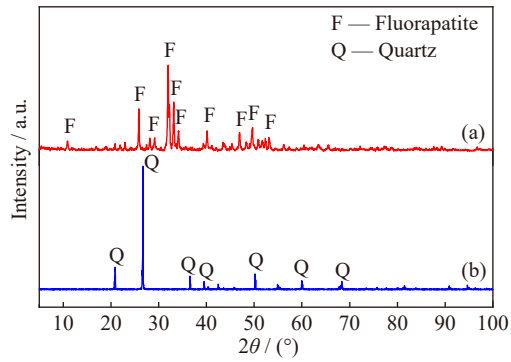

Fig. 3. X-ray diffractogram of (a) fluorapatite and (b) quartz.

Table 2. Chemical multi-element analysis results of pure mineral wt%

Mineral	SiO_2	Al_2O_3	P_2O_5	CaO	Fe_2O_3	Cl
Quartz	99.37	0.21	0.04	0.36	0.01	0.01
Mineral	MgO	Al_2O_3	P_2O_5	CaO	Fe_2O_3	F
Fluorapatite	0.08	4.2	39.56	53.35	1.69	1.12

The AMICS process software was used to conduct the AMICS analysis for actual minerals. The mineral composition analysis results (Table 3) indicate that the main useful mineral in the actual minerals was fluorapatite (with a content of 60.96wt%). Meanwhile, the gangue minerals were mainly dolomite and quartz, with a high content (23.73wt% and 10.95wt%, respectively). Siliceous and magnesian gangue minerals must be effectively removed to obtain high-quality collophane concentrate.

Table 3. Relative contents of main minerals in flotation feed wt%

Fluorapatite	Dolomite	Quartz	Augite	Orthoclase	Kimzeyite	Armstrongite	Isokite	Calcite	Illite	Others
60.96	23.73	10.95	0.1	0.3	0.96	0.89	0.12	0.37	0.51	1.11

Fig. 4 shows the data of particle size distribution for the flotation feed obtained from the AMICS analysis. Particle sizes for d_{50}, d_{90}, and d_{95} (the particle size corresponding to the cumulative distribution of 50%, 90%, and 95%, respectively) were 35.26, 100.52, and 122.75 μm, respectively. The liberation data obtained from the AMICS analysis (Fig. 5) indicate that the flotation feed was not fully liberated (particles with a liberation degree greater than 90% were considered

liberated particles). The liberated collophane particles accounted for only 65.30wt% of all particles. Meanwhile, the liberation degree of dolomite and quartz was only 47.24wt% and 43.63wt%, respectively.

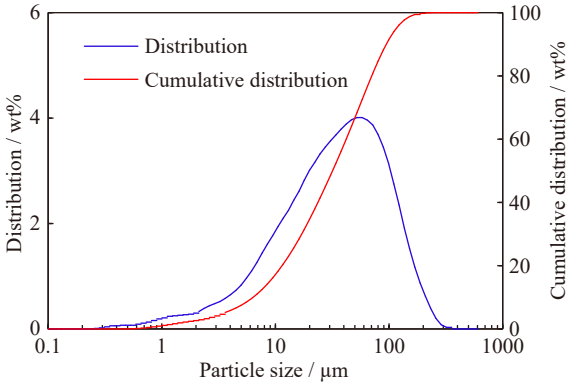

Fig. 4. Size distribution of flotation feed.

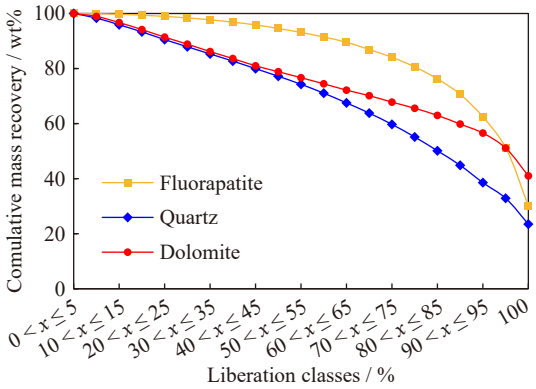

Fig. 5. Liberation degree of major minerals in flotation feed.

3.2. Flotation tests

3.2.1. Microflotation of pure minerals

The collector dosage or concentration and solution pH value considerably affect the potency and selectivity of the collector in a flotation process. The effect of the collector dosage and pH value on the floatability of pure quartz and fluorapatite must be investigated. The microflotation tests were conducted under the collector concentration of 0–500 mg·L^{-1} and pH value of 4–12. The obtained values were similar to the values for conditions employed by Li *et al.* [17] and Fang *et al.* [18] to compare the performance of the KDJ collector with that of the conventional collector. The floatability of pure quartz and fluorapatite is shown in Fig. 6 as a function of the collector concentration of 10–200 mg·L^{-1} and pH value of 4–12. Fig. 6(a) shows that the recoveries of both quartz and fluorapatite increased, corresponding to the increase in collector concentration at pH = 6. However, the effect of the collector concentration on the recovery of fluorapatite was negligible. Fluorapatite demonstrated no visible floatability when the collector concentration was less than 50 mg·L^{-1}. Thus, its flotation recovery curve was not noticeable in Fig. 4(b). Although the collector concentration increased to 200 mg·L^{-1}, the fluorapatite recovery was only approximately 20wt%. When the collector concentration increased from 10 to 25 mg·L^{-1}, the recovery of quartz increased from 77.86wt% to 97.83wt%. When the collector concentration exceeded 25 mg·L^{-1}, the recovery of quartz remained constant at about 98wt%.

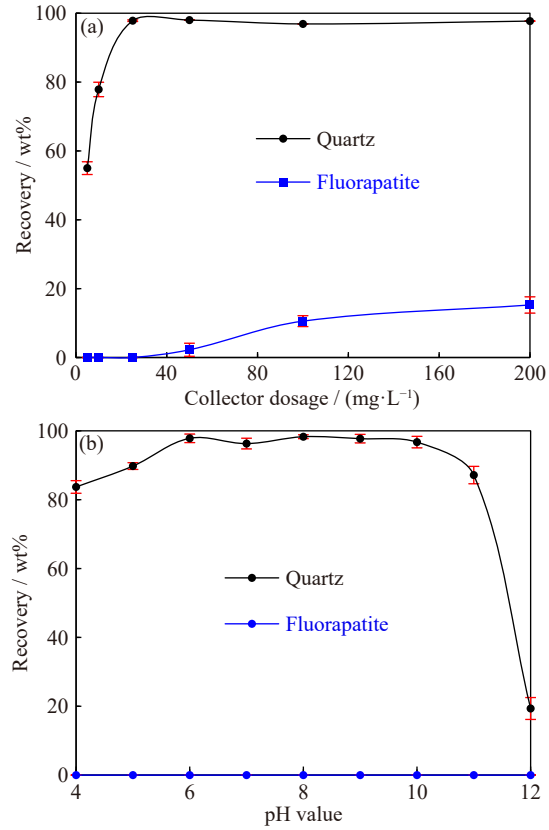

Fig. 6. Effect of collector dosage (at pH = 6) (a) and solution pH value (at collector dosage of 25 mg·L^{-1}) (b) on the floatability of quartz and fluorapatite. Fluorapatite flotation recovery in (b) was close to zero and thus not well shown in the figure.

The adsorption density of a cationic collector on the quartz surface increased with increasing collector concentration, whereas the adsorption on the fluorapatite surface remained low [17–19]. Thus, selective flotation separation was accomplished. However, when the cationic collector concentration was very high, a significant amount of the collector might also become adsorbed on collophane [20].

Fig. 6(b) shows the floatability of both pure quartz and fluorapatite at a collector concentration of 25 mg·L^{-1} as a function of pH. The figure also indicates that fluorapatite showed no floatability over the pH range of 4–10, but quartz showed strong floatability. The recovery of quartz increased with an increase in pH value and maintained a relatively high value of approximately 98wt% over the pH value of 6–10.

Fang *et al.* [18] showed that the low negative charge on the quartz surface at pH < 6 resulted in weak electrostatic adsorption between the collector and quartz. The negative charge on the quartz surface increased at a pH greater than 10, which should have enhanced the electrostatic adsorption of the collector for quartz. However, quartz recovery decreased when pH value increased above 10. This is due to low concentrations of ionic collector species at extremely

high pH value [21].

Previous studies have found that the optimum pH value for separating quartz from collophane was approximately pH value of 8 [1,11,18]. Li *et al.* [17] examined an amine collector for desilication from collophane under acidic pH. Quartz recovery was approximately 90wt%, and collophane recovery was 10wt%–20wt% over a wide range of pH values (4–10) at a collector concentration of 160 mg·L^{-1}. However, the novel KDJ collector not only reduced the collector dosage from 160 to 25 mg·L^{-1}, but it also showed better selectivity by facilitating approximately 100wt% recovery of quartz and no recovery of fluorapatite. Therefore, it exhibited greater collecting potency, higher selectivity, and better suitability for acidic conditions as compared to the conventional collector.

3.2.2. Flotation of actual minerals

Fig. 7 shows the flotation concentrate P_2O_5 and SiO_2 grade (left ordinate) and P_2O_5 recovery (right ordinate) as a function of the collector dosage at pH = 6 (Fig. 7(a)) and as a function of pH value at a collector dosage of 0.4 kg·t^{-1} (Fig. 7(b)). The results were obtained with the actual mineral sample in the second reverse flotation for desilication, as discussed in Section 2.2.3.

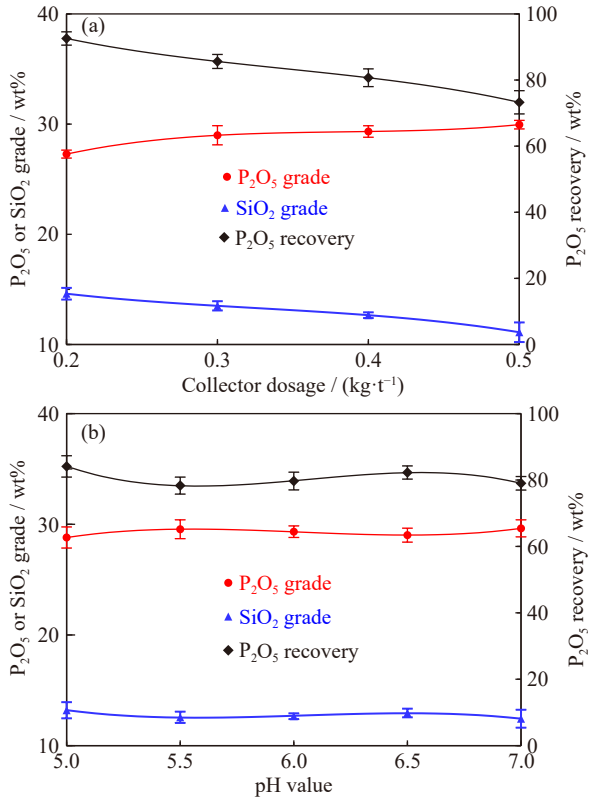

Fig. 7. Effects of collector dosage (at pH = 6) (a) and pH value (at collector dosage of 0.4 kg·t^{-1}) (b) on the floatability of actual minerals of quartz and collophane.

Fig. 7(a) shows that increasing the KDJ collector dosage from 0.2 to 0.5 kg·t^{-1} increased the P_2O_5 grade from 27.28wt% to 29.95wt%. However, it decreased the SiO_2 grade from 14.61wt% to 11.11wt% and the P_2O_5 recovery from 92.57wt% to 73.26wt%. The results indicate that the KDJ collector dosage exhibited significant influences on the flotation performance. This is consistent with the principle involved in the desilication process of collophane by reverse flotation. The optimum collector dosage was 0.4 kg·t^{-1} due to the reasonable compromise between P_2O_5 grade and recovery. Fig. 7(b) indicates that the required concentrate specifications of P_2O_5 grade <29wt% and SiO_2 grade <13wt% can be met by using the KDJ collector as the collophane desilication reagent by the double reverse flotation process in the pH value range of 5.5–7.0. The test results demonstrate that the effects of the collector dosage and pH value on the actual mineral flotation performance were essentially the same as those observed from microflotation tests with pure mineral samples. Further, the most appropriate pH value for the desilication reverse flotation was 6.0, which was identical to the slurry pH value used in the first reverse flotation process for magnesium removal. Therefore, the need to adjust the slurry pH value was eliminated, reducing the operating complexity and costs without sacrificing the process performance.

These data indicate that the new collector produced a concentrate with the specifications of P_2O_5 grade <29wt% and SiO_2 grade <13wt% under appropriate conditions. For example, a concentrate with 29.33wt% P_2O_5 grade and 12.66wt% SiO_2 content was generated at 80.69wt% P_2O_5 recovery with a collector dosage of 0.4 kg·t^{-1} at pH = 6. The flotation process under these conditions resulted in a P_2O_5 enrichment ratio of 1.12 and a SiO_2 removal of 46.45wt%. Zhao *et al.* [22] used a new collector coded GH-YH to desiliconize collophane by reverse flotation in the weakly alkaline pulp. They obtained a SiO_2 removal of only 8.22wt% at a P_2O_5 enrichment ratio of 1.05. Luo *et al.* [23] developed a novel collector coded AY suitable for use in a weak acidic pulp. Their test results showed that the reagent removed only 21.41wt% SiO_2 and achieved a P_2O_5 enrichment ratio (the ratio of concentrate grade to feed grade) of 1.06. These data analyses and performance comparisons demonstrate that the new KDJ collector was suitable for weakly acidic conditions, demonstrating high collecting potency and selectivity.

The relatively low P_2O_5 recovery observed in this study was consistent with that of previous studies. Wu and Tao [24] studied the process mineralogy of a similar collophane sample from Yunnan and its flotation separation difficulties. They concluded that the fine dissemination particle size of collophane, poor degree of mineral liberation, and serious slime generation were the main reasons for the poor flotation performance. This was exemplified by the fact that 4.74wt% liberated collophane particles of less than 30 μm were lost to the siliceous tailings in the closed-circuit double reverse desilication flotation process using a scavenger. Hoang *et al.* [25] claimed that the negative rheological effects within the pulp led to serious nonselective hydraulic entrainment of fine particles.

Existing studies show that nanobubble application in fine and ultrafine particle flotation can significantly improve the flotation efficiency, kinetics, and enrichment ratio and can reduce the consumption of collectors due to the unique characteristics of nanobubbles [26–29]. Tao *et al.* [30] and Sobhy

et al. [31] investigated nanobubble-enhanced reverse flotation of hematite for desilication. They concluded that cavitation-induced nanobubbles were preferentially generated on the surface of hydrophobic quartz particles, causing selective hydrophobic agglomeration. This was an effective method to improve fine particle separation. Therefore, using nanobubble flotation can improve the desilication performance of fine and ultrafine collophane particles.

3.3. Zeta potential measurements

Infrared spectrum analysis demonstrated that the KDJ collector adsorbed on quartz through physical adsorption but did not show adsorption on fluorapatite. In physical adsorption, the pH value of the pulp affects the surface charge of particles, affecting the adsorption of the collector on mineral surfaces. Therefore, we used a zeta potential measurement to explain the flotation separation behavior and synergistic effect between the two components in the KDJ collector. Fig. 8 shows the zeta potential measurement for quartz and fluorapatite in deionized water, CTAB solution, and KDJ collector solution at different pH values.

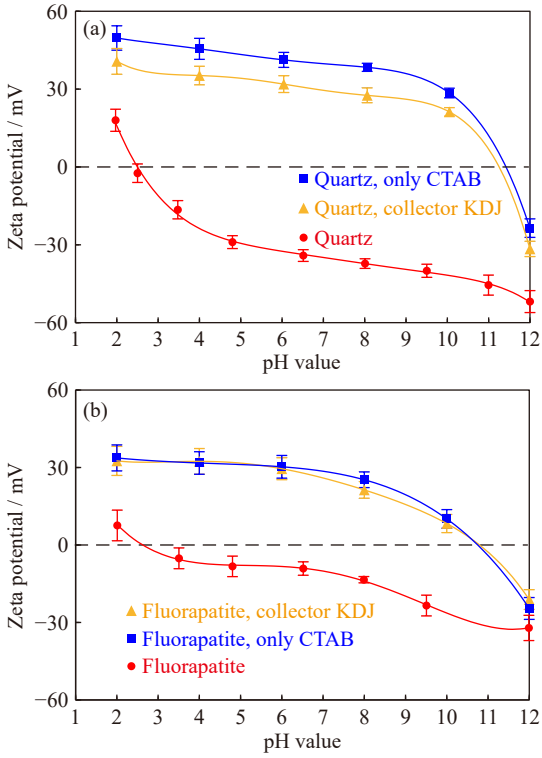

Fig. 8. Zeta potentials of quartz (a) and fluorapatite (b) as a function of pH value in deionized water, 50 mg·L^{-1} CTAB solution (without DBP), and 50 mg·L^{-1} collector KDJ solution.

As shown in Fig. 8, the natural zeta potential of both quartz and fluorapatite decreased and became negative when the pH value in deionized water increased. Moreover, quartz demonstrated more negative zeta potentials than that demonstrated by fluorapatite in the pH value range of 2–12. The isoelectric point of quartz and fluorapatite was approximately 2.56 mV and 2.60 mV, respectively, which is consistent with those in previous studies [32–33].

The surface potential of quartz and fluorapatite after treatment with the two tested collectors changed considerably to positive values, indicating the adsorption of the collectors on the quartz and fluorapatite surfaces. In the presence of CTAB, the surface potential of quartz and fluorapatite decreased from 49.70 and 33.70 mV to −23.58 and −24.58 mV, respectively, when the pH value increased from 2 to 12. Cationic collectors are often adsorbed on the surface of quartz and collophane through electrostatic adsorption [17–18,34]. However, the cationic collector is preferentially adsorbed on the negatively charged surface of quartz than that of the fluorapatite. This is because the quartz surface has a greater negative charge than that on the fluorapatite surface. The negative charge is essential for the effective separation of quartz from collophane [17].

In the presence of the KDJ collector with the CTAB and DBP, the surface potential was between 40.70 and −31.58 mV and between 32.56 and −21.13 mV for quartz and fluorapatite, respectively, over the same pH value range of 2–12. The comparison between the two curves obtained with the KDJ collector and CTAB clearly indicates that the DBP introduction in the KDJ collector shifted the surface potential of quartz to low positive or high negative values. However, it did not significantly affect the surface potential of fluorapatite as the two curves in the presence of KDJ and CTAB were identical for fluorapatite. Liu *et al.* [35–36] and Sun *et al.* [37] reported that nonpolar compounds (e.g., dodecane, kerosene, and polyethylene glycol sorbitan monooleate) showed a strong negative zeta potential. Therefore, DBP was selectively adsorbed on the surface of hydrophobic quartz than that of fluorapatite. Wu *et al.* [38] examined the synergistic effect of DBP with CTAB, which is similar to that of the major components of the KDJ collector, on the flotation separation of quartz from fluorapatite. They observed that when CTAB and DBP were mixed before adding to the pulp, CTAB was adsorbed on DBP droplets with the hydrocarbon chain of CTAB extending into DBP droplets and its polar head exposed to the solution. In addition, the free DBP droplets function as a bridge between CTAB and quartz particles. Therefore, the presence of DBP in the KDJ collector resulted in considerable differences in the adsorption of CTAB on quartz and fluorapatite, which created favorable conditions for separating fluorapatite from quartz.

3.4. Infrared spectroscopic analysis

We analyzed the infrared spectra of quartz and fluorapatite before and after interactions with the new collector to analyze the adsorption mechanisms at pH = 6. As shown in Fig. 9, the characteristic peaks for pure quartz appeared from 400 to 1100 cm^{-1}. The peaks at 1083.85 cm^{-1} and 786.75 cm^{-1} were attributed to the asymmetric and symmetrical stretching vibration of Si–O, respectively. Moreover, the peaks at 686.54 cm^{-1} and 461.54 cm^{-1} were attributed to the symmetrical bending vibration of Si–O and the asymmetrical bending vibration of Si–O–Si [39]. After conditioning with the KDJ collector, the characteristic peak of quartz did not

shift. However, two absorption peaks of the hydrocarbon chain group were observed at 2923.75 cm^{-1} and 2856.20 cm^{-1}. Hence, the physical adsorption of the KDJ collector on the surface of quartz conforms with the result of the zeta potential measurement.

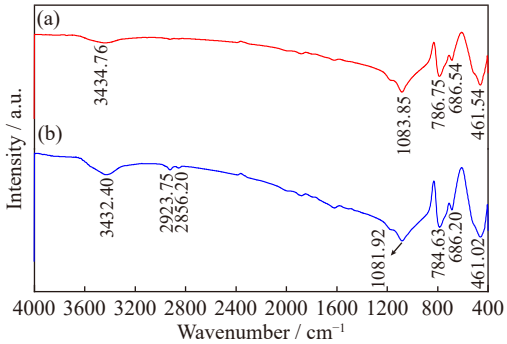

Fig. 9. Infrared spectra of quartz: (a) pure; (b) conditioned with KDJ at pH = 6.

Fig. 10 shows the infrared spectra of fluorapatite before and after treatment with the KDJ collector. The characteristic peaks of pure fluorapatite appeared from 400 to 1100 cm^{-1}. The doublet of 1096.34 cm^{-1} and 1045.28 cm^{-1} was assigned to the asymmetric stretching vibration of P–O, and that at 605.57 cm^{-1} and 568.93 cm^{-1} was ascribed to the bending vibration of P–O [32]. As shown by curve (b) in Fig. 10, neither a new absorption peak of the functional group nor a characteristic peak of the KDJ collector appeared on the surface of fluorapatite after treatment with the collector. Further, the characteristic peaks of pure fluorapatite did not visibly shift, indicating that the KDJ collector has no adsorption on the fluorapatite surface. The adsorption mechanism of the KDJ collector on fluorapatite observed from infrared spectrum tests does not conform with its zeta potential measurements. Therefore, electrostatic attraction between the KDJ collector and fluorapatite is extremely weak, and the adsorbed collector can be removed by washing it with deionized water. This demonstrates that the KDJ collector adsorption on quartz and fluorapatite surfaces is considerably different.

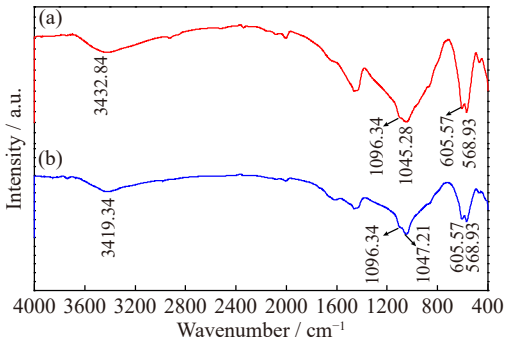

Fig. 10. Infrared spectra of fluorapatite: (a) mineral only; (b) conditioned with KDJ at pH = 6.

3.5. CA analysis

The flotation test results with pure minerals and actual ores indicate that the KDJ collector effectively separated quartz from fluorapatite. The adsorption of the collector greatly affects the hydrophobicity of mineral surfaces measured by the CA value [40]. We analyzed the CA of quartz and fluorapatite particles before and after treatment with the KDJ collector under the optimum flotation conditions to study the mechanisms of the high flotation performance achieved in the presence of the new collector.

Fig. 11 shows the CA of quartz and fluorapatite before and after treatment with the KDJ collector at pH = 6.0. The natural CA of quartz and fluorapatite was 7.4° and 26.2°, respectively, conforming with the CA values from existing studies [18,41]. After treatment with the KDJ collector, the CA of quartz increased sharply to 62.5°, whereas that of fluorapatite changed marginally to 30.9°.

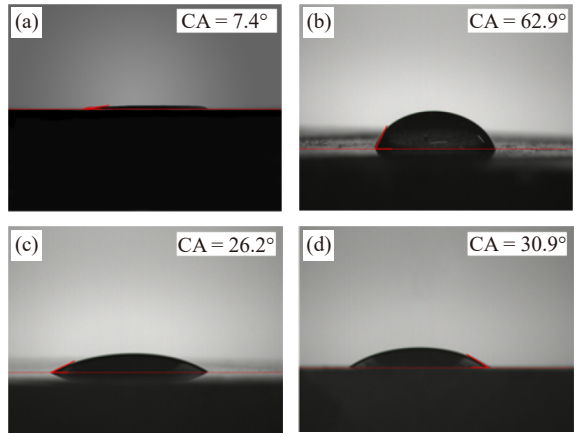

Fig. 11. CA measurement results with pure minerals: (a) quartz; (b) quartz conditioned with collector; (c) fluorapatite; (d) fluorapatite conditioned with collector.

In general, a CA of less than 45° denotes weak hydrophobicity, and a CA considerably greater than 45° denotes strong hydrophobicity, making particles easily floatable [33]. Fang *et al.* [18] investigated the effect of ether amine collector on the CA of quartz and fluorapatite (collophane). They reported that the CA of fluorapatite (collophane) was approximately 35° while the CA of quartz was nearly 60°. Li *et al.* [17] showed that the CA of quartz and fluorapatite was 54° and 34°, respectively, at an optimum pH value of 7 in the presence of a 200 $mg \cdot L^{-1}$ AY collector, resulting in the best flotation performance. An analysis of the CA measurement for different collectors for reverse flotation of collophane clearly demonstrates that the new KDJ collector exhibits the greatest capability of increasing the CA difference between quartz and fluorapatite. Therefore, the KDJ collector exhibits unique selectivity and great potential for improving the flotation performance of collophane for quartz removal.

3.6. Froth stability characterization

Froth stability in the presence of collectors is an important parameter in the flotation process. It is often measured by the defoaming rate, defined as the slope on the curve of froth volume as a function of time (Fig. 12). The initial froth volume in this study was 163 mL.

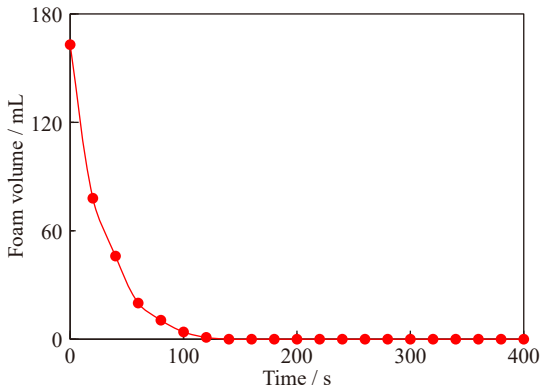

Fig. 12. Froth volume as a function of time.

As shown in Fig. 12, the froth volume decreased with time due to the continuous coalescence of air bubbles. The defoaming rate was 142.8 mL·min^{-1} in the first 60 s. Moreover, only 20 mL of froth remained after 60 s, and the froth disappeared completely after approximately 120 s. Ji *et al.* [42] investigated the defoaming effect of defoamer CA-2035 on the desilication of collophane by reverse flotation. They concluded that adding an 800 g·t^{-1} defoamer improved the defoaming rate by approximately three times without affecting the collecting performance of the dodecylamine collector. The defoaming rate was 73.3 mL·min^{-1} in the presence of 800 g·t^{-1} defoamer CA-2035. This is considerably lower than the defoaming rate observed in Fig. 12 without using a defoamer. Moreover, the froth generated in the presence of the KDJ collector did not encounter the defoaming difficulties often encountered with conventional collectors for collophane desilication flotation. Liu *et al.* [34] and Wu *et al.* [38] analyzed the synergistic effect between nonpolar surfactants and the cationic amine collector. They concluded that the surface tension of a mixed reagent solution decreases when surfactants are added. For example, the introduction of 20 mg·L^{-1} DBP reduced the γ_{CMC} (surface tension under the critical micelle concentration) of CTAB solution with a concentration of 100 mg·L^{-1} from 40.9 to 28.7 mN·m^{-1}, as reported by Wu *et al.* [38]. The KDJ collector was a mixture of CTAB and DBP, and its surface tension was considerably lower than that of conventional amine collectors. Flotation is a complex physical and chemical process in a three-phase system, particularly for the mineralization and defoaming processes. The wetting work of a solid–liquid interface expressed in Eq. (1) is often used to explain the effect of surface tension on the defoaming process.

$$W = \gamma(1 + \cos\theta) \quad (1)$$

where W is the wetting work, J; γ is surface tension of collector, mN·m^{-1}; θ is contact angle, (°). Eq. (1) shows that wetting work W decreases with decreasing surface tension γ and increasing contact angle θ due to the addition of a frother and a collector, respectively. Zhou *et al.* [43] showed that kerosene droplets enhanced coalescence and reduced the stability of bubbles. Xu *et al.* [44] demonstrated that the oil bridge formed by diesel droplets dispersed in the middle of the foam film caused the foam film rupture through the single foam film drainage tests. The spreading pressure of the oil film increased with an increase in diesel concentration. The competitive adsorption between diesel droplets and frother molecules reduced the effective concentration of frother at the gas–water interface. Similar mechanisms may be responsible for the rapid defoaming phenomenon caused by the KDJ collector.

4. Conclusions

We successfully used the new cationic collector KDJ for effective desilication of collophane by reverse flotation at a weakly acidic pH value of 6.0. This pH value was identical to that used in a previous flotation process for magnesium removal. The micro-flotation tests demonstrated that the KDJ collector exhibited strong collecting potency, excellent selectivity, and great adaptability in a wide pH range of 4–10. The flotation tests with an actual mineral sample demonstrated that a single stage of the reverse flotation process with a 0.4 kg·t^{-1} KDJ collector at pH = 6 generated a concentrate of 29.33wt% P_2O_5 grade with 12.66wt% SiO_2 at a P_2O_5 recovery of 79.69wt%. These values were significantly better than those for existing cationic collectors used for collophane desilication.

The infrared spectrum analysis and zeta potential indicated the electrostatic adsorption of the KDJ collector on quartz and collophane. KDJ exhibited a good affinity to the strongly negatively charged surface of the quartz. Moreover, the difference in hydrophobicity between quartz and collophane increased for KDJ. The defoaming performance in the presence of KDJ was far better compared with that of conventional traditional collectors. Hence, the need for a defoamer was eliminated.

Acknowledgements

The authors acknowledge the financial support from the National Natural Science Foundation of China (No. 51804188) and the support of the Yunnan Yuntianhua Co., Ltd., China, for providing the phosphate samples.

Conflict of Interest

The authors declare that they have no known competitive financial interests or personal relationships that could affect the work reported in this paper.

References

[1] Z.Q. Huang, C. Cheng, Z.W. Liu, *et al.*, Utilization of a new Gemini surfactant as the collector for the reverse froth flotation of phosphate ore in sustainable production of phosphate fertilizer, *J. Clean. Prod.*, 221(2019), p. 108.
[2] Food and Agriculture Organization of the United Nation, *World Fertilizer Trends and Outlook to 2022*, Rome, 2019, p. 2.
[3] B. Geissler, M.C. Mew, O. Weber, and G. Steiner, Efficiency performance of the world's leading corporations in phosphate rock mining, *Resour. Conserv. Recycl.*, 105(2015), p. 246.
[4] M. Mohammadkhani, M. Noaparast, S.Z. Shafaei, A. Amini, E. Amini, and H. Abdollahi, Double reverse flotation of a very low

grade sedimentary phosphate rock, rich in carbonate and silicate, *Int. J. Miner. Process.*, 100(2011), No. 3-4, p. 157.
[5] X. Liu, C.X. Li, H.H. Luo, R.J. Cheng, and F.Y. Liu, Selective reverse flotation of apatite from dolomite in collophanite ore using saponified gutter oil fatty acid as a collector, *Int. J. Miner. Process.*, 165(2017), p. 20.
[6] D.H. Hoang, N. Kupka, U.A. Peuker, and M. Rudolph, Flotation study of fine grained carbonaceous sedimentary apatite ore – Challenges in process mineralogy and impact of hydrodynamics, *Miner. Eng.*, 121(2018), p. 196.
[7] B. Feng, L.Z. Zhang, W.P. Zhang, H.H. Wang, and Z.Y. Gao, Mechanism of calcium lignosulfonate in apatite and dolomite flotation system, *Int. J. Miner. Metall. Mater.*, 29(2022), No. 9, p. 1697.
[8] H.Y. Yang, J.F. Xiao, Y. Xia, *et al*., Origin of the Ediacaran Weng'an and Kaiyang phosphorite deposits in the Nanhua Basin, SW China, *J. Asian Earth Sci.*, 182(2019), art. No. 103931.
[9] A. Abdelkrim, B. Mustapha, and S. Kouachi, Two-stage reverse flotation process for removal of carbonates and silicates from phosphate ore using anionic and cationic collectors, *Arab. J. Geosci.*, 11(2018), No. 19, art. No. 593.
[10] C.H. Du, Y.Y. Ge, and M. Liu, Study on double reverse flotation of silicon-calcareous (magnesium) phosphate ore from Guizhou, *Met. Mine*, 2019, No. 1, p. 92.
[11] S.B. Liu, Y.Y. Ge, J. Fang, J. Yu, and Q. Gao, An investigation of froth stability in reverse flotation of collophane, *Miner. Eng.*, 155(2020), art. No. 106446.
[12] M.A. Zhou, C. Dai, L.F. Liu, and S.X. Fang, Reconstruction of flotation column in Kunyang phosphate flotation plant, *Modern Min.*, 32(2016), No. 6, p. 75.
[13] W.B. Liu, W.G. Liu, D.Z. Wei, M.Y. Li, Q. Zhao, and S.C. Xu, Synthesis of N,N-Bis(2-hydroxypropyl)laurylamine and its flotation on quartz, *Chem. Eng. J.*, 309(2017), p. 63.
[14] P. de Oliveira, H. Mansur, A. Mansur, G. da Silva, and A.E. Clark Peres, Apatite flotation using pataua palm tree oil as collector, *J. Mater. Res. Technol.*, 8(2019), No. 5, p. 4612.
[15] Y.L. Botero, R. Serna-Guerrero, A. López-Valdivieso, M. Benzaazoua, and L.A. Cisternas, New insights related to the flotation of covellite in porphyry ores, *Miner. Eng.*, 174(2021), art. No. 107242.
[16] E. Sadeghinezhad, M.A.Q. Siddiqui, H. Roshan, and K. Regenauer-Lieb, On the interpretation of contact angle for geomaterial wettability: Contact area versus three-phase contact line, *J. Pet. Sci. Eng.*, 195(2020), art. No. 107579.
[17] X.B. Li, Q. Zhang, B. Hou, J.J. Ye, S. Mao, and X.H. Li, Flotation separation of quartz from collophane using an amine collector and its adsorption mechanisms, *Powder Technol.*, 318(2017), p. 224.
[18] J. Fang, Y.Y. Ge, and J. Yu, Adsorption behavior and mechanism of an ether amine collector on collophane and quartz, *Physicochem. Probl. Miner. Process.*, 55(2019), No. 1, p. 301.
[19] W.B. Liu, W.X. Huang, F. Rao, Z.L. Zhu, Y.M. Zheng, and S.M. Wen, Utilization of DTAB as a collector for the reverse flotation separation of quartz from fluorapatite, *Int. J. Miner. Metall. Mater.*, 29(2022), No. 3, p. 446.
[20] Z.Q. Huang, S.Y. Zhang, H.L. Wang, *et al*., "Umbrella" structure trisiloxane surfactant: Synthesis and application for reverse flotation of phosphorite ore in phosphate fertilizer production, *J. Agric. Food Chem.*, 68(2020), No. 40, p. 11114.
[21] C.Y. Sun and W.Z. Yin, *Flotation Principles of Silicate Minerals*, Science Press, Beijing, 2001, p. 127.
[22] F.T. Zhao, R.L. Li, L.F. Liu, and L.L. Zhang, Discussion on double-reverse flotation desilication process of carbonate collophanite in Yunnan, *Ind. Miner. Process.*, 48(2019), No. 8, p. 48.
[23] J.Y. Luo, *Study on Double Reverse Flotation of Desilication of Micro-fine Phosphate Ore* [Dissertation], Guizhou University, Guizhou, 2018, p. 56.
[24] Z.X. Wu and D.P. Tao, Mineralogical analysis of collophane in Yunnan using AMICS and exploration of difficult flotation mechanisms, *Chin. J. Eng.*, 43(2021), No. 4, p. 503.
[25] D.H. Hoang, A. Hassanzadeh, U.A. Peuker, and M. Rudolph, Impact of flotation hydrodynamics on the optimization of fine-grained carbonaceous sedimentary apatite ore beneficiation, *Powder Technol.*, 345(2019), p. 223.
[26] F.Y. Ma, D.P. Tao, and Y.J. Tao, Effects of nanobubbles in column flotation of Chinese sub-bituminous coal, *Int. J. Coal Prep. Util.*, 42(2022), No. 4, p. 1126.
[27] D.P. Tao and A. Sobhy, Nanobubble effects on hydrodynamic interactions between particles and bubbles, *Powder Technol.*, 346(2019), p. 385.
[28] F.Y. Ma, P. Zhang, and D.P. Tao, Surface nanobubble characterization and its enhancement mechanisms for fine-particle flotation: A review, *Int. J. Miner. Metall. Mater.*, 29(2022), No. 4, p. 727.
[29] C.W. Li, D.L. Li, X. Li, M. Xu, and H.J. Zhang, Surface nanobubbles on the hydrophobic surface and their implication to flotation, *Int. J. Miner. Metall. Mater.*, 29(2022), No. 8, p. 1493.
[30] D.P. Tao, Z.X. Wu, and A. Sobhy, Investigation of nanobubble enhanced reverse anionic flotation of hematite and associated mechanisms, *Powder Technol.*, 379(2021), p. 12.
[31] A. Sobhy, Z.X. Wu, and D.P. Tao, Statistical analysis and optimization of reverse anionic hematite flotation integrated with nanobubbles, *Miner. Eng.*, 163(2021), art. No. 106799.
[32] J. Angélica Evangelista de Carvalho, P. Roberto Gomes Brandão, A. Bicalho Henriques, P. Silva de Oliveira, R. Zanoni Lopes Cançado, and G. Rodrigues da Silva, Selective flotation of apatite from micaceous minerals using patauá palm tree oil collector, *Miner. Eng.*, 156(2020), art. No. 106474.
[33] Y. Han, S. Han, B. Kim, *et al*., Flotation separation of quartz from apatite and surface forces in bubble-particle interactions: Role of pH and cationic amine collector contents, *J. Ind. Eng. Chem.*, 70(2019), p. 107.
[34] A. Liu, P.P. Fan, X.X. Qiao, Z.H. Li, H.F. Wang, and M.Q. Fan, Synergistic effect of mixed DDA/surfactants collectors on flotation of quartz, *Miner. Eng.*, 159(2020), art. No. 106605.
[35] A. Liu, M.Q. Fan, Z.H. Li, and J.C. Fan, Non-polar oil assisted DDA flotation of quartz I: Interfacial interaction between dodecane oil drop and mineral particle, *Int. J. Miner. Process.*, 168(2017), p. 1.
[36] A. Liu, M.Q. Fan, and P.P. Fan, Interaction mechanism of miscible DDA-Kerosene and fine quartz and its effect on the reverse flotation of magnetic separation concentrate, *Miner. Eng.*, 65(2014), p. 41.
[37] W.H. Sun, W.G. Liu, S.J. Dai, T. Yang, H. Duan, and W.B. Liu, Effect of Tween 80 on flotation separation of magnesite and dolomite using NaOL as the collector, *J. Mol. Liq.*, 315(2020), art. No. 113712.
[38] Z.X. Wu, D.P. Tao, P. Zhang, X.J. Jiang, and M. Jiang, Synergistic effect of DBP with CTAB on flotation separation of quartz from collophane, *Minerals*, 11(2021), No. 11, art. No. 1196.
[39] W.G. Liu, W.B. Liu, X.Y. Wang, D.Z. Wei, and B.Y. Wang, Utilization of novel surfactant N-dodecyl-isopropanolamine as collector for efficient separation of quartz from hematite, *Sep. Purif. Technol.*, 162(2016), p. 188.
[40] Z.L. Zhu, D.H. Wang, B. Yang, *et al*., Effect of nano-sized roughness on the flotation of magnesite particles and particle-bubble interactions, *Miner. Eng.*, 151(2020), art. No. 106340.
[41] Y.H. Wang and J.W. Ren, The flotation of quartz from iron minerals with a combined quaternary ammonium salt, *Int. J. Miner. Process.*, 77(2005), No. 2, p. 116.
[42] B. Ji, W. Sun, and R.L. Wang, Defoaming mechanism in reverse flotation of collophanite using dodecyl amine, *Min. Metall. Eng.*, 38(2018), No. 2, p. 47.
[43] S.Q. Zhou, X.X. Wang, X.N. Bu, *et al*., Effects of emulsified kerosene nanodroplets on the entrainment of gangue materials and selectivity index in aphanitic graphite flotation, *Miner. Eng.*, 158(2020), art. No. 106592.
[44] M.D. Xu, Y.W. Xing, W. Jin, M. Li, Y.J. Cao, and X.H. Gui, Effect of diesel on the froth stability and its antifoam mechanism in fine coal flotation used MIBC as the frother, *Powder Technol.*, 364(2020), p. 183.